Molecular Pharmacology Fast Forward. Published on March 25, 2019 as DOI: 10.1124/mol.118.114389
This article has not been copyedited and formatted. The final version may differ from this version.

MOL # 114389

TITLE PAGE

Characterization of 6-mercaptopurine transport by the SLC43A3-encoded nucleobase transporter

Nicholas Ruel, Khanh H. Nguyen, Gonzalo Vilas, James R. Hammond

Department of Pharmacology, University of Alberta, Edmonton, Alberta, Canada T6G 2H7

Molecular Pharmacology Fast Forward. Published on March 25, 2019 as DOI: 10.1124/mol.118.114389
This article has not been copyedited and formatted. The final version may differ from this version.

RUNNING TITLE PAGE

a) Running Title: Cellular uptake of 6-mercaptopurine

b) Corresponding author:

Dr James R Hammond

Department of Pharmacology

9-70 Medical Sciences Building

University of Alberta

Edmonton, AB T6G 2H7 Canada

Email: james.hammond@ualberta.ca

Tel: 780-492-3414 Fax: 780-492-4325

c) #Text pages = 40

#Tables = 1

#Figures = 10

#References = 40

Abstract = 250 words

Introduction = 625 words

Discussion = 1505 words

Molecular Pharmacology Fast Forward. Published on March 25, 2019 as DOI: 10.1124/mol.118.114389
This article has not been copyedited and formatted. The final version may differ from this version.

d) Abbreviations

6-MP – 6-mercaptopurine

6-TG – 6-thioguanine

CNT2 – concentrative nucleoside transporter 2

CNT3 – concentrative nucleoside transporter 3

D22 – Decynium-22

DMSO – dimethyl sulfoxide

DY – dipyridamole

ENBT1 – equilibrative nucleobase transporter 1

ENT1 – equilibrative nucleoside transporter 1

ENT2 – equilibrative nucleoside transporter 2

ENT4 – equilibrative nucleoside transporter 4

HPRT - Hypoxanthine-guanine phosphoribosyltransferase

MMP – 6-methylmercaptopurine

MTT - (3-(4,5-Dimethylthiazol-2-yl)-2,5-Diphenyltetrazolium Bromide)

MTX – methotrexate

NBMPR – nitrobenzylthioinosine

NMG – N-methylglucamine

OAT1 – organic anion transporter 1

OAT3 – organic anion transporter 3

TPMT – thiopurine methyltransferase

e) Recommended section: Metabolism, Transport, and Pharmacogenomics

Molecular Pharmacology Fast Forward. Published on March 25, 2019 as DOI: 10.1124/mol.118.114389
This article has not been copyedited and formatted. The final version may differ from this version.

ABSTRACT

6-Mercaptopurine (6-MP) is a nucleobase analog used in the treatment of acute lymphoblastic leukemia and inflammatory bowel disorders. However, the mechanisms underlying its transport into target cells have remained elusive. The protein encoded by SLC43A3_1 (ENBT1) has recently been shown to transport endogenous nucleobases. A splice variant (SLC43A3_2), encoding a protein with 13 additional amino acids in the first extracellular loop, is also expressed but its function is unknown. We hypothesized that 6-MP is a substrate for both variants of ENBT1. HEK293 cells (lacking endogenous ENBT1 activity) were transfected with each of the coding region variants of SLC43A3. ENBT1 function was assessed via the rate of flux of [^{3}H]adenine and [^{14}C]6-MP across the plasma membrane. Both SLC43A3 variants encoded proteins with similar functional properties. [^{14}C]6-MP and [^{3}H]adenine had K_m values (±SD) of 163 ± 126 μM and 37 ± 26 μM, respectively, for this system. Decynium-22, 6-thioguanine and 6-methylmercaptopurine inhibited 6-MP uptake with K_i values of 1.0 ± 0.4, 67 ± 30, and 73 ± 20 μM, respectively. ENBT1 also mediated adenine-sensitive efflux of 6-MP from the SLC43A3-HEK293 cells. MRP4 also contributed to the efflux of 6-MP in this model, but was less efficient than ENBT1 in this regard. Furthermore, transfection of HEK293 cells with SLC43A3 increased the sensitivity of the cells to the cytotoxic effects of 6-MP by more than 7-fold. Thus, both variants of ENBT1 are key players in the transfer of 6-MP into and out of cells, and changes in SLC43A3 expression impacts 6-MP cytotoxicity.

Molecular Pharmacology Fast Forward. Published on March 25, 2019 as DOI: 10.1124/mol.118.114389
This article has not been copyedited and formatted. The final version may differ from this version.

INTRODUCTION

Nucleobase analogue drugs are used as antiviral and anticancer agents, with one of the most established being 6-mercaptopurine (6-MP), used in the maintenance phase of therapy for acute lymphoblastic leukemia (ALL). These compounds are generally pro-drugs in that they need to be metabolized by intracellular enzymes to their active phosphorylated derivatives. The first step in this activation process is the transport of the nucleobase analogues into the target cells.

A number of different mechanisms have been proposed for the cellular entry of nucleobase analogues. Early studies suggested that SNBT1, a sodium dependent nucleobase transporter identified in porcine LLC-PK1 cells, was the 6-MP transporter (Griffith and Jarvis, 1993). However, this was found to be a defective pseudogene in humans (Yamamoto et al., 2010), and is thus not relevant to the clinical actions of these agents. OAT1 and OAT3 have also been shown to mediate the transport of nucleobase drugs such as 6-MP (Mori et al., 2004), but these transporters are limited in their expression profile and are notably absent in leukemia cells (Burckhardt, 2012). The nucleoside transporters hENT1 and hENT2 can also transport nucleobases including 6-MP, but with low affinity (K_m values greater than 1 mM; 1000-fold higher than therapeutic levels of 6-MP) (Yao et al., 2011). An earlier study using mouse ENT2-overexpressing Cos-7 cells reported that 6-MP had a 14 μM K_m for ENT2(Nagai et al., 2007), suggesting that there may be species differences in ENT2 affinity for 6-MP. In 2007, we characterized a novel nucleobase transport system in human cardiac microvascular endothelial cells and gave it the designation ENBT1 (Equilibrative Nucleobase Transporter 1)(Bone and Hammond, 2007). Using transporter-selective inhibitors, we determined that ENBT1 was distinct from any of the aforementioned putative nucleobase transporters, and was blocked by nucleobase analogues such as 6-MP and 6-thioguanine (6-TG) at concentrations in the low micromolar

Molecular Pharmacology Fast Forward. Published on March 25, 2019 as DOI: 10.1124/mol.118.114389
This article has not been copyedited and formatted. The final version may differ from this version.

range. We also described ENBT1 activity in a variety of other cell lines including U2OS, UMR, MDCK, PK15-NTD, rMVEC, but, notably, not in HEK293 cells (Bone and Hammond, 2007). However, the gene encoding ENBT1 was not known at that time and, other than our group subsequently showing that ENBT1 could be modulated by oxidative stress in an ischemia-reperfusion injury model(Bone et al., 2014), no further analysis was done. In late 2015, SLC43A3, an orphan member of the amino acid transporter gene family (Bodoy et al., 2013), was shown to encode a protein that led to the cellular uptake of the nucleobases adenine and hypoxanthine when expressed in MDCKII cells (Furukawa et al., 2015), with characteristics almost identical to those that we described previously for ENBT1(Bone and Hammond, 2007). Those investigators also showed that the SLC43A3-encoded transporter could be inhibited by 6-MP. SLC43A3 is expressed at low to moderate levels in most tissues, including bone marrow, and has been identified in myeloid and lymphoid cell lines (Human Protein Atlas)(Thul et al., 2017). None of the aforementioned studies, however, considered the fact that SLC43A3 exists as multiple splice variants. Many of the variants differ in the 5'-UTR, but two encode full length proteins that differ in the absence (SLC43A3_1) or presence (SLC43A3_2) of a 13 amino acid insert in the first predicted extracellular loop (Fig 1). The study examining recombinant SLC43A3 expression in MDCKII cells used the isoform 1 variant (Furukawa et al., 2015). There have been no studies done on the functional characteristics of the protein encoded by SLC43A3_2, nor has 6-MP actually been shown to be a substrate for either of these transporter variants. If the two SLC43A3 isoforms differ in function or substrate selectivity, their differential expression in cells may impact the effectiveness of nucleobase analogue drug substrates. We report herein on the characteristics of adenine and 6-MP transport by the ENBT1 variants encoded by SLC43A3_1 and SLC43A3_2 expressed in HEK293 cells.

Molecular Pharmacology Fast Forward. Published on March 25, 2019 as DOI: 10.1124/mol.118.114389
This article has not been copyedited and formatted. The final version may differ from this version.

MATERIALS AND METHODS

Materials. [2,8-^{3}H]adenine (20-40 Ci/mmol), [8-^{14}C]-6-MP (50-60 mCi/mmol), and [^{3}H]water (1 mCi/g) were from Moravek Biochemicals (Brea, CA). 6-TG, hypoxanthine, 6-methylmercaptopurine (MMP), 2-chloroadenosine, adenine, adenosine, 3-(4,5-dimethyl-2-thiazolyl)-2,5-diphenyl-2H-tetrazolium bromide (MTT), nitrobenzylthioinosine (NBMPR), dipyridamole (DY), geneticin (G418), DMEM, and amphotericin B were purchased from Sigma-Aldrich (St. Louis, MO). Calf serum was from GE Healthcare Hyclone (Logan, UT). All primers were ordered through Integrated DNA Technologies (Coralville, Iowa). Agarose, oligo $(dT)_{12\text{-}18}$ primer, and M-MLV Reverse Transcriptase came from Invitrogen (Burlington, ON). The 100 bp DNA Ladder was supplied by Truin Science (Edmonton, AB). Power Up SYBR Green and TRIzol Reagent was supplied by Life Technologies (Burlington, ON). Antibodies used included mouse monoclonal anti-Myc (Clone 4A6, 05-724, Lot #2585792; EMD Millipore, Canada), rabbit polyclonal anti-SLC43A3 (HPA030551, Lot #R31257; Sigma-Aldrich, St. Louis, MO), mouse monoclonal anti-β-actin (C4, sc-47778, Lot #D1713; Santa Cruz Biotechnology Inc., Texas, USA). HRP-conjugated secondary antibodies (Donkey anti-rabbit IgG-HRP, sc-2313, Lot #LK0312) and m-IgGk (BP-HRP, sc-516102, Lot #F1016) were also purchased from Santa Cruz Biotechnology. Decynium-22 (D22), ceefourin-1, and zaprinast were from Tocris Bioscience (Oakville, ON), and methotrexate (MTX) was from Alfa Aesar (Tewksbury, MA). HEK293 cells were purchased from ATCC (Manassas, Virginia, USA).

Myc-SLC43A3 plasmid construct. Oligonucleotides corresponding to the coding region of isoform 1 (NM_001278201) or isoform 2 (NM_001278206) of SLC43A3, with an N-terminal myc-epitope tag, were prepared in the GeneArt Cloning pMA plasmid by Invitrogen. The Myc-

Molecular Pharmacology Fast Forward. Published on March 25, 2019 as DOI: 10.1124/mol.118.114389
This article has not been copyedited and formatted. The final version may differ from this version.

SLC43A3 sequences were transferred to the mammalian cloning vector pcDNA3.1 (-) using the Xbal (5') and KpnI (3') restriction enzymes. The inserts were sequenced in both directions to confirm integrity and then used to transfect HEK293 cells using the calcium phosphate method(Kingston et al., 2003). Cells expressing SLC43A3 were selected based on their resistance to 600 µg/ml G418 using standard procedures. Cells stably transfected with the 'empty' pcDNA3.1 vector were also tested to assess the impact of the transfection procedure and G418 on the measured parameters.

Cell Culture. HEK293 cells were cultured in DMEM with 5% calf serum, 5% fetal bovine serum, penicillin (100 units/mL), streptomycin (100 µg/mL), sodium pyruvate (1 mM), and amphotericin B (0.5 µg/mL). G418 was added (120 µg/ml) in the SLC43A3-HEK293 cell media to maintain selection pressure on the stable transfectants. The HEK293 cells were removed from flasks by exposure to 0.05% trypsin/EDTA for 10 min at 37°C and the suspended cells washed in the appropriate buffer solution (without G418) immediately prior to use in subsequent assays.

PCR. Cells from confluent 10 cm plates were suspended in 1 ml of TRIzol reagent and homogenized for extraction of RNA according to the manufacturer's protocol (Invitrogen). Total RNA concentration and purity was determined using a Nanodrop 2000 spectrophotometer (Life Technologies Inc., Burlington, ON, Canada). For qualitative PCR, 5 µg of Total RNA was reverse transcribed to cDNA using Oligo $(dT)_{12-18}$ primer and M-MLV reverse transcriptase, and amplified using recombinant Taq DNA Polymerase (Thermo Scientific Canada) and primers designed for SLC43A3 (forward primer: 5'- GGAACTCCGCTCCTTCT; reverse primer 3'- TGATCACTTGCAGGATGAAG), or GAPDH (forward primer: 5'- ACATCATCCCTGCCTCTAC; reverse primer 3'- CCTGTTGCTGTAGCCAAAT). Primer

Molecular Pharmacology Fast Forward. Published on March 25, 2019 as DOI: 10.1124/mol.118.114389
This article has not been copyedited and formatted. The final version may differ from this version.

efficiency and melt curves were assessed prior to their use for gene expression analysis. The following conditions were used for amplification: 3 min at 95 °C followed by 40 cycles of 30 s at 95 °C, 30 s at 56°C, 60 s at 72°C, followed by extension for 10 min at 72°C in a BioRad T-100 Thermocycler. Semi-quantitative PCR (qPCR) was conducted using cDNA (~100 ng/well) prepared as described above with the primer sets shown in (Supplemental Table 1) using Power Up SYBR Green fluorescence on a Roche Light Cycler 480 System (Cardiovascular Research Centre, Edmonton, Canada). qPCR conditions were: 2 min at 50°C (UDG activation), 2 min at 95°C (denaturation) followed by 45 cycles of 15 s at 95°C, 60 s at 60°C for amplification, with a final melt curve analysis. Gene expression was normalized to glyceraldehyde 3-phosphate dehydrogenase (GAPDH) and analyzed relative to expression in the un-transfected HEK293 cells using the ΔΔCt method. GAPDH Ct values were relatively consistent across the cell models used (18.8 ± 0.2, 19.4 ± 0.3, 16.9 ± 0.3, and 19.0 ± 0.3 for the un-transfected HEK293 cells and the cells transfected with pcDNA3.1, SLC43A3_1 and SLC43A3_2, respectively, n=5).

Immunoblotting: Samples were prepared in RIPA buffer (150 mM NaCl, 50 mM Tris, 1% NP-40, 0.5% sodium deoxycholate, 1% SDS) containing protease inhibitors. Samples were adjusted to 2% (v/v) β-mercaptoethanol, and resolved by SDS-PAGE on 12.5% (w/v) acrylamide gels. Proteins were electro-transferred onto Immobilon-P PVDF membranes (Millipore Corporation, MA, USA) for 1.5 hr at a constant current of 280 mA. After transfer, membranes were rinsed in Tris buffered saline (TBS; 0.15 M NaCl, 50 mM Tris, pH 7.5) and incubated with TBS-TM (TBS containing 0.2% v/v Tween-20 and 5% w/v skim milk powder) for 1 hr at room temperature with gentle rocking to block nonspecific binding. Membranes were then incubated for 16 hr at 4°C with gentle rocking in the presence of either mouse anti-Myc, rabbit anti-SLC43A3, or mouse anti-β-actin at 1:1000, 1:250 and 1:500 dilutions, respectively, in TBS-TM (containing 1% skim milk).

Molecular Pharmacology Fast Forward. Published on March 25, 2019 as DOI: 10.1124/mol.118.114389
This article has not been copyedited and formatted. The final version may differ from this version.

After successive washes with TBS-TM (containing 1% skim milk), the membranes were incubated with a 1:5000 or 1:3000 dilution of donkey anti-rabbit IgG-HRP or m-IgGk BP-HRP, respectively, in TBS-TM for 1 hr at room temperature and further washed with TBS-T (TBS, containing 0.2% (v/v) Tween-20). Proteins were detected using ECL western blot substrate (EMD Millipore, Canada) and visualized using a ChemiDoc™ XRS + System (Bio-Rad Laboratories, Canada).

Nucleobase Uptake. Cells were suspended in nominally sodium-free buffer (to eliminate any potential contribution of sodium-dependent transporters) (NMG buffer; 140 mM N-methylglucamine, 5 mM KCl, 4.2 mM $KHCO_3$, 0.36 mM K_2HPO_4, 0.44 mM KH_2PO_4, 10 mM HEPES, 0.5 mM $MgCl_2$, 1.3 mM $CaCl_2$, pH 7.4) containing 500 nM DY (to block potential ENT1/ENT2-mediated uptake) for 15 min at room temperature prior to assay. Cellular uptake was initiated by adding 250 µl of cell suspension to 250 µl of [^{14}C]6-MP or [^{3}H]adenine layered over 21:4 silicone:mineral oil (v:v) (200 µl) in 1.5 ml microcentrifuge tubes. The uptake reaction was terminated after specified times by centrifugation of the cells through the oil layer at ~10,000 *g*. The aqueous layer was aspirated and upper tube washed with ~1 ml of NMG buffer prior to removal of the oil layer. The resulting cell pellet was digested in 1 M NaOH overnight (~16 hr), with aliquots of digested cells assessed for radioactive content using standard liquid scintillation counting techniques in a Beckman Coulter LS6500 scintillation system. Non-mediated uptake was defined as uptake of [^{3}H]adenine by un-transfected HEK293 cells, or uptake of [^{14}C]6-MP by cells in the presence of 1 mM adenine. Mediated-uptake was defined as the difference between the total uptake and non-mediated uptake components. Cell volume (µl) was estimated by incubating cells with [^{3}H]water for 3 min, centrifuging the cells through the oil layer, sampling 100 µl of the supernatant and processing as above. Total cellular water volume was determined from the ratio of the dpm of the cell pellet to the dpm of the supernatant, allowing for

Molecular Pharmacology Fast Forward. Published on March 25, 2019 as DOI: 10.1124/mol.118.114389
This article has not been copyedited and formatted. The final version may differ from this version.

inter-experimental normalization via calculation of pmol of substrate accumulated per µl of cell-associated water.

6-MP Efflux. Cells were removed from confluent T175 flasks and suspended in sodium free buffer as described for the nucleobase uptake assays. Cell number was determined using Trypan Blue Stain (Hyclone, GE Healthcare, Logan, UT) on a BioRad TC10 Automated Cell Counter prior to loading the cells with radioactive substrate. Cells were loaded with 100 µM [^{14}C]6-MP for 30 s and then centrifuged at 1000 g for 30 s to lightly pellet the cells. Supernatant was removed and cell pellets rapidly suspended in sodium-free buffer (± inhibitors) to initiate efflux. Aliquots (500 µl) of this cell suspension were layered over 21:4 silicone:mineral oil (v:v) in a 1.5 ml microcentrifuge tube and centrifuged at specified time points. The cell pellets were then washed and incubated in 1 M NaOH overnight and processed as described for the nucleobase uptake assays for determination of intracellular [^{14}C] content. In experiments where 1 mM adenine was used, the initial load of [^{14}C]6-MP (time 'zero') was determined by extrapolation of the exponential decay curve fit to the data obtained in the presence of 1 mM adenine. In experiments where 1 mM adenine was not used, the initial load of [^{14}C]6-MP (time 'zero') was determined by centrifuging an aliquot (500 µl) of the cells immediately following the loading step and processing as described above. No difference was noted between these two methods in determination of initial load for these experiments.

Cell Viability. Cells were seeded into a 24 well plate at a density of 5 x 10^4 cells/well in culture media and allowed to attach overnight. Culture media was removed the following day and replaced by media containing 6-MP (75 nM-1.28 mM) and incubated for 48 hr at 37°C in a humidified 5% CO_2 atmosphere. In some cases, the ENT1/ENT2 inhibitor DY or the MRP4 and

Molecular Pharmacology Fast Forward. Published on March 25, 2019 as DOI: 10.1124/mol.118.114389
This article has not been copyedited and formatted. The final version may differ from this version.

MRP5 inhibitors ceefourin-1 and zaprinast, respectively, were included in the media to assess the influence of these transporters on 6-MP cytotoxicity. After 48 hr the media was removed and replaced with D-PBS (137 mM NaCl, 2.7 mM KCl, 6.3 mM Na_2HPO_4, 1.5 mM KH_2PO_4, 0.5 mM $MgCl_2 \cdot 6H_20$, 0.9 mM $CaCl_2 \cdot 2H_20$, pH 7.4) containing MTT (1 mg/ml) for 90 min. Formazan crystals formed were solubilized in 450 µl of DMSO and absorbance was measured at 570 nm in a Spectra Max 340 plate reader (Molecular Devices, Sunnyvale, CA).

Data analysis and statistics. Data are expressed as mean ± SD. Sample size was pre-determined as N=5 (5 independent experiments with 2-3 internal replicates); that is the minimum needed to define statistical differences based on the known historical variability inherent in these types of studies. In some circumstances, where higher variability was seen due to methodological issues (e.g. the rapid uptake profiles using the HEK293-SLC443A3_1 cells), an additional 1 or 2 experiments were added. Nonlinear curves were fitted to data, and statistical analyses done, using GraphPad Prism 8.01 software. In all cases, if the P value determined from a statistical test was less than 0.5, the difference was considered significant and the null-hypothesis (no difference between data sets) rejected. Efflux data were assessed using both one-phase decay and two-phase decay profiles and the curve that fit best to the data was determined by the F-test. Influx data were best represented by a one-phase association profile (versus two-phase). Significant differences between groups were assessed using Student's t-test, corrected for multiple comparisons with the Holm-Sidak method. For inhibition analyses, K_i values were determined from IC_{50} values, using the specified substrate concentration [S], based on the Cheng-Prusoff equation: $K_i = IC_{50}/(1 + [S]/K_m)$ (Cheng and Prusoff, 1973) using the respective K_m values for 6-MP transport determined in this study.

Molecular Pharmacology Fast Forward. Published on March 25, 2019 as DOI: 10.1124/mol.118.114389
This article has not been copyedited and formatted. The final version may differ from this version.

RESULTS

Transfection of HEK293 cells with SLC43A3. To ensure that our stable cell transfection protocol was successful, qualitative PCR was conducted using cDNA prepared from un-transfected HEK293 and SLC43A3-transfected HEK293 cells (Fig. 2A). The un-transfected and vector-only transfected HEK293 cells expressed minimal levels of SLC43A3 isoform 1, and there was no detectable isoform 2 transcript, supporting prior data showing that these cells do not have measurable ENBT1-mediated nucleobase flux capacity (Bone and Hammond, 2007). In contrast, the SLC43A3-transfected cell lines expressed high levels of the SLC43A3 transcript (Fig 2A). Both SLC43A3 isoform-encoded proteins were also detected by immunoblotting using either anti-SLC43A3 (Fig 2B) or anti-myc (Fig 2C) antibodies, with about 6-fold more isoform 1 detected than isoform 2 (relative to β-actin). We will henceforth refer to the encoded proteins as ENBT1.1 (isoform 1) and ENBT1.2 (isoform 2).

Gene expression analysis. The more sensitive qPCR analyses indicated that HEK293 cells did express low levels of SLC43A3, but the SLC43A3_1 transfected and SLC43A3_2 transfected cells had more than 3240-fold and 840-fold higher levels of the respective transcript than un-transfected HEK293 cells (Fig 3A). Interestingly, cells stably transfected with the empty vector, pcDNA3.1, showed a 10-fold decrease in endogenous SLC43A3 expression (Fig 3A). To determine if transfection of HEK293 cells with SLC43A3, or the vector alone, led to compensatory changes in other relevant genes, we examined the level of expression of the nucleoside transporters SLC29A1 (ENT1), SLC29A2 (ENT2), and SLC29A4 (ENT4), the efflux pumps ABCC4 (MRP4) and ABCC5 (MRP5), and the intracellular enzymes involved in 6-MP metabolism, thiopurine methyltransferase (TPMT) and hypoxanthine-guanine

Molecular Pharmacology Fast Forward. Published on March 25, 2019 as DOI: 10.1124/mol.118.114389
This article has not been copyedited and formatted. The final version may differ from this version.

phosphoribosyltransferase (HPRT). ABCC5 was downregulated, and TPMT and HPRT were upregulated, in the vector transfected cells (Fig 3B). In contrast, in cells transfected with SLC43A3, the transcripts for SLC29A2, ABCC4, and ABCC5 were found to be downregulated in both the SLC43A3_1-transfected cells (Fig 3C) and SLC43A3_2-transfected (Fig 3D) cells relative to control HEK293 cells. In addition, the SLC43A3_2 transfected cells showed a significant decrease in SLC29A4 transcript (Fig 3D). No changes were noted for the other transcripts measured.

[^{3}H]Adenine influx. Un-transfected HEK293 cells, or cells transfected with empty vector, exhibited minimal time-dependent uptake of [^{3}H]adenine (Fig 4A&B), In contrast, [^{3}H]adenine influx by cells transfected with SLC43A3_1 was time-dependent with steady state accumulation of 100 µM [^{3}H]adenine (67 ± 11 pmol/µl) achieved within 10 s (Fig 4A), reflecting the high level of expression of ENBT1.1 in these cells (see Fig 2). When the background (un-transfected HEK293 cell-associated [^{3}H]adenine) was subtracted, an initial rate of ENBT1.1-mediated transport of 18 ± 9 pmol/µl/s (for 100 µM [^{3}H]adenine) was estimated by extrapolation of the uptake profile to 0.5 s. The transport efficiency of this system made it necessary to conduct full time courses at each substrate concentration to allow determination of transporter kinetics based on initial rates (estimated from uptake at 0.5 s derived from curves fitted to each independent experiment). In contrast, ENBT1.2-mediated [^{3}H]adenine influx in the SLC43A3_2 transfected cells was slower with an initial rate for 100 µM [^{3}H]adenine influx of 6 ± 2 pmol/µl/s (Fig 4B), reflecting the relatively lower level of ENBT1.2 protein in the transfected HEK293 cells (Fig 2B). Thus, initial rates for ENBT1.2-mediated influx were estimated from the experimentally-determined 2 s uptake time point. The results of these kinetic experiments are shown in Fig. 4C.

Molecular Pharmacology Fast Forward. Published on March 25, 2019 as DOI: 10.1124/mol.118.114389
This article has not been copyedited and formatted. The final version may differ from this version.

[^{3}H]Adenine transport by ENBT1.1 had a K_m of 37 ± 26 μM and a V_{max} of 34 ± 6 pmol/μl/s. ENBT1.2 had a K_m for adenine (40 ± 26 μM) similar to that of ENBT1.1 and a V_{max} of 7.9 ± 1.6 pmol/μl/s.

ENBT1-mediated [^{14}C]6-MP influx. Similar studies were then conducted using [^{14}C]6-MP as the substrate. As seen for the [^{3}H]adenine uptake assays, the 'background' uptake of [^{14}C]6-MP in the un-transfected HEK293 cells was higher than expected for this assay protocol. However, this background was not affected by addition of the ENT1/ENT2 inhibitor DY (1 μM) (Ward et al., 2000), the pan-nucleoside transporter substrate uridine (1 mM)(Young et al., 2013), nor the nucleobase adenine (1 mM), indicating it was not due to the operation of other nucleoside/nucleobase transporters such as ENT1, ENT2, CNT3 that have been suggested by others to mediate 6-MP uptake (Nagai et al., 2007; Yao et al., 2011). Nor did the organic anion transporter (OAT) inhibitor novobiocin (300 μM)(Mori et al., 2004; Duan and You, 2009; Burckhardt, 2012) have an effect on this residual accumulation of 100 μM 6-MP (17.8 ± 1.8 pmol/μl/2 s and 17.2 ± 1.8 pmol/μl/2 s in the absence and presence of novobiocin, respectively, N=5). Nor was the background reduced by additional washing steps, suggesting that this remaining [^{14}C] was likely cell membrane-associated [^{14}C]6-MP or nonspecific binding of [^{14}C]6-MP to the polypropylene centrifuge tubes. HEK293 cells expressing ENBT1.1 accumulated 100 μM 6-MP in a time-dependent manner, and this uptake could be inhibited completely by 1 mM adenine (Fig 5A). Fig 5B shows a similar time course profile for 30 μM 6-MP uptake by un-transfected and pcDNA3.1-transfected HEK293 cells, and ENBT1.2-expressing HEK293 cells in the presence and absence of 1 mM adenine. As for the ENBT1.1 expressing cells (Fig 5A), the uptake of 6-MP by the ENBT1.2 expressing cells was inhibited

Molecular Pharmacology Fast Forward. Published on March 25, 2019 as DOI: 10.1124/mol.118.114389
This article has not been copyedited and formatted. The final version may differ from this version.

completely by 1 mM adenine, with the uptake in the presence of adenine not significantly different from 6-MP uptake by the un-transfected HEK293 cells or the vector-only transfected cells (Fig 5B). Therefore, 6-MP uptake in the presence of 1 mM adenine was defined as non-transporter-mediated background in subsequent experiments. Time courses of uptake by ENBT1.1 were constructed for a range of [^{14}C]6-MP concentrations (1-300 μM), with initial rates represented by the rate of influx at 0.5 s extrapolated from individual time course curves. ENBT1.1-mediated [^{14}C]6-MP accumulation was saturable with a K_m of 163 ± 126 μM and a V_{max} of 82 ± 30 pmol/μl/s (Fig. 5C). ENBT1.2-expressing cells accumulated [^{14}C]6-MP at less than half the rate of ENBT1.1-transfected cells (Vmax = 32 ± 8 pmol/μl/s), again reflecting the lower expression level of ENBT1.2 relative to ENBT1.1. However, the K_m of [^{14}C]6-MP for ENBT1.2 mediated transport (188 ± 68 μM) was not significantly different from that determined for ENBT1.1.

Inhibition of ENBT1-mediated 6-MP uptake. A number of compounds were screened initially at a single concentration for their ability to inhibit the 2 s influx of [^{14}C]6-MP in the ENBT1.1 (Fig 6A) and ENBT1.2 (Fig 6B) expressing HEK293 cells. All inhibitors tested affected ENBT1.1 and ENBT1.2 mediated 6-MP uptake similarly. The nucleoside adenosine (1 mM) did not affect 6-MP uptake. Nor did MTX, a folate analogue that is used concurrently with 6-MP in the treatment of ALL. However, the adenosine analogue 2-chloroadenosine did produce a significant inhibition of 6-MP uptake (58 ± 6% inhibition of ENBT1.1 at 1 mM). NBMPR, the selective ENT1 nucleoside transport inhibitor, inhibited ENBT1.1 mediated 6-MP uptake by 41% at 100 μM. As has been shown previously (Furukawa et al., 2015), D22 was a relatively effective inhibitor of ENBT1 achieving 71 ± 6% inhibition of ENBT1.1 at 10 μM. The

Molecular Pharmacology Fast Forward. Published on March 25, 2019 as DOI: 10.1124/mol.118.114389
This article has not been copyedited and formatted. The final version may differ from this version.

nucleobases 6-TG and hypoxanthine, at 1 mM, inhibited 100 μM [^{14}C]6-MP uptake by ENBT1.1 by 86 ± 14% and 61 ± 6%, respectively. The 6-MP metabolite 6-methylmercaptopurine (MMP) also inhibited ENBT1.1-mediated 6-MP uptake by 91 ± 6% at 1 mM. 6-TG is a nucleobase analogue similar in structure to 6-MP. Therefore, it is anticipated that 6-TG may also be a substrate for ENBT1 and, as such, should act as a competitive inhibitor of 6-MP for the substrate recognition site. To test this, we examined the uptake of a range of concentrations of [^{3}H]adenine by ENBT1.1 in the presence of 750 μM 6-TG (Fig. 6C). [^{3}H]Adenine uptake in the presence of 6-TG had a significantly higher apparent K_m with no significant difference in V_{max} relative to data obtained in the absence of 6-TG (see Fig 4C), indicative of competitive inhibition kinetics. Full concentration-inhibition profiles were then constructed for 6-TG, MMP, and D22 (Fig. 6D) allowing the calculation of K_i values of 67 ± 30, 73 ± 20, and 1.0 ± 0.4 μM, respectively, for their inhibition of 6-MP uptake by ENBT1.1.

ENBT1-mediated 6-MP efflux. To determine whether ENBT1 was bidirectional with respect to the transport of 6-MP, SLC43A3_1-transfected HEK293 cells were loaded with 100 μM [^{14}C]6-MP for 30 s and assessed for the rate of release of [^{14}C] upon resuspension of cells in substrate free media. The change in intracellular 6-MP was measured with time after resuspension (Fig 7). Due to the handling time required for this experimental procedure, the minimum efflux time that could be reliably attained was 10 s. From the data shown in Fig. 7 it is apparent that, in the absence of any competing compound, a new steady-state was achieved prior to the first recordable time point of 10 s (estimated rate constant of at least 0.35 s^{-1}). This rapid rate of efflux was not unexpected given the rapid rate of 6-MP influx by ENBT1.1 in this recombinant transfection model (see Fig. 5A). The presence of extracellular adenine decreased

Molecular Pharmacology Fast Forward. Published on March 25, 2019 as DOI: 10.1124/mol.118.114389
This article has not been copyedited and formatted. The final version may differ from this version.

the rate of 6-MP efflux significantly. The efflux time course in the presence of 1 mM adenine fit best to a one-phase decay profile, allowing the calculation of an efflux rate constant of 0.020 ± 0.004 s^{-1}. Efflux in the presence of 100 μM adenine fit best to a two-phase decay profile with the first phase having a rate constant of 0.15 ± 0.10 s^{-1}, and the second phase having a rate constant of 0.014 ± 0.016 s^{-1}, which is not significantly different from the rate of efflux in the presence of 1 mM adenine. When the same type of analysis was done using un-transfected HEK293 cells, it was necessary to use a 10 min loading time for [^{14}C]6-MP to achieve comparable intracellular concentrations to those seen using the 30 s loading time in the SLC43A3 transfected cells. Efflux of 6-MP from the HEK293 cells was dramatically slower that that observed in the SLC43A3 transfected cells, with over 70% of the initial load still retained within the cell after 3 min. Adenine (1 mM) had a slight, but significant, inhibitory effect on this [^{14}C]6-MP efflux from the un-transfected HEK293 cells (rate constants of 0.14 ± 0.08 s^{-1} and 0.07 ± 0.04 s^{-1} in the absence and presence of adenine, respectively) suggesting that it was mediated by endogenous nucleobase transporters.

Given the two-phase decay profile observed in the presence of 100 μM adenine, and the finding that ABCC4, ABCC5, and SLC29A2 expression all declined concomitant with the increased expression of SLC43A3_1 by the HEK293 cells (Fig 3C), we examined the effect of the ABCC4 inhibitor ceefourin-1, the ABCC5 inhibitor zaprinast, and the SLC29A2 inhibitor DY on the efflux of 6-MP from the SLC43A3_1 transfected cells (Fig 8). Ceefourin-1 had no significant effect on the initial rate of 6-MP efflux in the absence of adenine (0.29 ± 0.16 s^{-1} and 0.38 ± 0.86 s^{-1}, in the absence and presence of ceefourin-1, respectively) (Fig 8A). However, ceefourin-1 did reveal a second slower phase of efflux with a rate constant of 0.02 ± 0.04 s^{-1}. The rapidity of the

Molecular Pharmacology Fast Forward. Published on March 25, 2019 as DOI: 10.1124/mol.118.114389
This article has not been copyedited and formatted. The final version may differ from this version.

efflux in the absence of adenine made these data difficult to interpret due to the large errors on the calculated parameters. Therefore, the effect of ceefourin-1 was also assessed in combination with 100 μM adenine. Efflux in the presence of 100 μM adenine was monophasic in this case with a rate constant of 0.16 ± 0.04 s^{-1}, similar to the first phase of efflux in the presence of 100 μM adenine seen previously as reported in Fig 7. Addition of ceefourin-1 led to a biphasic efflux profile with the initial fast component having a rate constant of 0.26 ± 0.24 s^{-1} (which is not significantly different than that seen in the absence of ceefourin-1), and a significantly larger slower component with a rate constant of 0.014 ± 0.014 s^{-1}. In the absence of ceefourin-1, 75 ± 2% of the efflux occurred at the faster rate in the presence of 100 μM adenine. However, in the presence of ceefourin-1, this initial fast component represented only 42 ± 18 % of the total efflux. In contrast, the ABCC5 inhibitor zaprinast had no significant effect on 6-MP efflux in either the presence or absence of 100 μM adenine (Fig 8B). Likewise, the combination of ceefourin-1 and zaprinast (Fig 8C) affected 6-MP efflux in a manner similar to that seen using ceefourin-1 alone. The SLC29A2 inhibitor DY also had no effect on the efflux of 6-MP (Fig 8D).

SLC43A3 expression and cell viability. If ENBT1 is critical to the cellular accumulation of 6-MP, and hence its cytotoxicity, then one might predict that the SLC43A3-transfected HEK293 cells would be more sensitive to the toxic effects of 6-MP than un-transfected HEK293 cells. In un-transfected HEK293 cells, 6-MP had a biphasic effect on cell viability with 51 ± 16% of the cells impacted by 6-MP with an EC_{50} of 5.6 μM ($logEC_{50}$ = -5.25 ± 0.16), while the remaining cells were relatively resistant to 6-MP with 35 ± 8% remaining even after 48 hr exposure to 1 mM 6-MP (Fig 9A). Cells transfected with the 'empty' pcDNA3.1 plasmid had a

Molecular Pharmacology Fast Forward. Published on March 25, 2019 as DOI: 10.1124/mol.118.114389
This article has not been copyedited and formatted. The final version may differ from this version.

similar biphasic profile with an EC_{50} of 13.2 μM ($LogEC_{50}$ = -4.878 ± 0.064) for 6-MP mediated cytotoxicity which is slightly, but significantly (Extra sum-of squares F test, $P<0.05$), higher than that seen for the un-transfected HEK293 cells (Fig 9A). Cells transfected with SLC43A3_1 and SLC43A3_2 also had biphasic responses to 6-MP. However, in both cases, there was a significantly lower proportion of 6-MP resistant cells after transfection with SLC43A3 (50 ± 26% and 23 ± 8% for un-transfected and SLC43A3_1 transfected cells, and 44 ± 14% and 28 ± 6% for un-transfected and SLC43A3_2 transfected HEK293 cells, respectively). Transfection of HEK293 cells with SLC43A3 also enhanced the sensitivity of the cells to the cytotoxic effects of 6-MP, by 7-fold (Fig 9A) and 15-fold (Fig 9B) for the SLC43A3_1 and SLC43A3_2 transfected cells, respectively. $LogEC_{50}$ values for 6-MP-mediated cytotoxicity of -6.05 ± 0.22 and -6.29 ± 0.06 were calculated from these data for the SLC43A3_1 and SLC43A3_2 transfected cells, respectively. To assess the contribution of the nucleoside/nucleobase transporters ENT1 and ENT2 to these actions of 6-MP, similar analyses were conducted in the presence and absence of DY (Fig 9C). DY, at concentrations sufficient to completely block ENT1 and ENT2 (1 μM), did not change the cytotoxicity profile of 6-MP in either the un-transfected or SLC43A3_1-transfected HEK293 cells. In addition, the inclusion of G418 in the media during the 48 hr cytotoxicity assay did not affect the sensitivity of either the SLC43A3_1- or the SLC43A3_2-transfected cells to 6-MP (Fig 9D)

To confirm that this increased sensitivity to 6-MP was due to the SLC43A3 transfection and not the concomitant decrease in MRP4 and MRP5 activity observed in the SLC43A3 isoform 1 transfected HEK293 cells (see Fig 3), these studies were repeated in the presence of the MRP4 and MRP5 inhibitors ceefourin-1 and zaprinast. These inhibitors, alone or in combination, had

Molecular Pharmacology Fast Forward. Published on March 25, 2019 as DOI: 10.1124/mol.118.114389
This article has not been copyedited and formatted. The final version may differ from this version.

no significant effect on the cytotoxic EC_{50} of 6-MP in un-transfected HEK293 cells (Fig 10A), or in cells transfected with SLC43A3_1 (Fig 10B) (e.g. logEC_{50} of 6-MP in HEK293 cells of -5.21 ± 0.08 and -5.17 ± 0.06 in the absence and presence of ceefourin+zaprinast, respectively). However, ceefourin-1 alone or in combination with zaprinast, did cause a significant increase in the relative proportion of 6-MP-resistant cells in the un-transfected HEK293 population (Fig 10A) (29 ± 2% and 40 ± 2% of the cells were resistant to 6-MP in the absence and presence of ceefourin/zaprinast, respectively). For the SLC43A3_1 transfected cells, while comparison of individual data points did not indicate any significant differences, curve analysis did show a similar significant shift in the resistant cell population upon treatment with the combination of ceefourin-1 and zaprinast (38 ± 2% and 49 ± 2% resistant cells in the absence and presence of the MRP inhibitors, respectively)(Fig 10B) . Suppression of ABCC4 expression (by ~60%; Fig 10D) by stable transfection of cells with ABCC4-targeted siRNA also led to a significant enhancement in the proportion of SLC43A3_1 transfected HEK293 cells resistant to 6-MP (26 ± 8% and 37 ± 6% without and with siRNA, respectively)(Fig 10C), but had no effect on the cytotoxic EC_{50} of 6-MP. However, siRNA suppression of ABCC4 in the un-transfected HEK293 cells actually led to a significant decrease in the proportion of cells resistant to 6-MP (44 ± 2% and 34 ± 2% without and with siRNA, respectively). There was also a significant enhancement in the cytotoxicity of 20 μM and 30 μM 6-MP in the siRNA transfected cells, but there was no change in the overall EC_{50} of 6-MP for the sensitive population of cells (due to the increase in the relative percentage of 6-MP sensitive cells after siRNA transfection).

Molecular Pharmacology Fast Forward. Published on March 25, 2019 as DOI: 10.1124/mol.118.114389
This article has not been copyedited and formatted. The final version may differ from this version.

DISCUSSION

Both isoforms of SLC43A3 encode proteins (ENBT1.1 and ENBT1.2) that mediate the uptake of the endogenous nucleobase adenine and the nucleobase analogue 6-MP with comparable K_m values (Figs 4C and 5C). Therefore, the 13 amino acid insert in the first extracellular loop of ENBT1.2 does not directly affect substrate affinity or transporter function. The K_m for adenine determined herein was similar to that reported for the SLC43A3_1-encoded ENBT1 expressed in MDCKII cells (Furukawa et al., 2015), and is also similar to that which we reported for an ENBT1-like transporter in human microvascular endothelial cells (Bone and Hammond, 2007). Transfection of HEK293 cells with SLC43A3 (either isoform) resulted in a dramatic enhancement in the ability of 6-MP to decrease cell viability (Fig 9). This indicates that ENBT1 activity has a direct impact on the cytotoxicity of 6-MP, and that variations in SLC43A3 expression may modify the therapeutic effectiveness of 6-MP. It is notable, however, that cells transfected with SLC43A3_2 had a similar shift in 6-MP cytotoxicity as cells transfected with SLC43A3_1, even though the level of transfection with SLC43A3_1 was 6-fold higher than that seen for SLC43A3_2 (Fig 2), and the SLC43A3_1 cells had an ~2.5-fold higher rate of uptake of 6-MP than the SLC43A3_2 cells (Fig 5C). This may indicate that ENBT1-mediated 6-MP transport is rate limiting for 6-MP cytotoxicity only up to a certain point, after which the intracellular metabolic pathways are saturated and the rate of 6-MP metabolism becomes limiting.

Stable transfection of HEK293 cells with SLC43A3 (either isoform) decreased the expression of SLC29A2 (ENT2), ABCC4 (MRP4) and ABCC5 (MRP5) (Fig 3C and D). Transfection with SLC43A3_2 also caused a downregulation of SLC29A4 (ENT4). The downregulation of

Molecular Pharmacology Fast Forward. Published on March 25, 2019 as DOI: 10.1124/mol.118.114389
This article has not been copyedited and formatted. The final version may differ from this version.

ABCC5 may due to the transfection or the influence of chronic exposure to G418, as a similar downregulation was seen in vector-only transfected cells (Fig 3B). The vector controls did not exhibit a downregulation of the other genes seen in the SLC43A3-transfected cells. The downregulation of ENT2 and MRP4 may reflect compensation by the cells to the enhanced availability of nucleobases via ENBT1 to support intracellular metabolism (Senyavina and Tonevitskaya, 2015). Both of these transporters are known to mediate the flux of 6-MP(Janke et al., 2008; Peng et al., 2008; Ansari et al., 2009; Yao et al., 2011; Tanaka et al., 2015). However, in terms of 6-MP sensitivity, a decrease in ENT2 activity would actually lead to reduced cellular uptake of 6-MP and, consequently, decreased cytotoxicity – opposite to that observed in the present study. hENT2 has a very low affinity for 6-MP (> 1 mM K_m) relative to ENBT1 (Yao et al., 2011) making it unlikely to contribute to 6-MP uptake at clinically relevant concentrations. Furthermore, we showed that the ENT1/ENT2 inhibitor DY impacted neither the uptake nor the efflux of 6-MP; nor did it affect 6-MP cytotoxicity. The reason for the downregulation of ENT4 in the SLC43A3_2 transfected cells is obscure. ENT4 is predominantly a monoamine transporter at neutral pH, and transports adenosine under acidic pH conditions (Zhou et al., 2007; Zhou et al., 2010), and nucleobases are not substrates for ENT4. On the other hand, the efflux pumps MRP4 and MRP5 are known to be associated with 6-MP resistance (Chen et al., 2001; Reid et al., 2003; Fukuda and Schuetz, 2012), and their decreased expression was thus considered a potential factor in the increased 6-MP cytotoxicity observed. The MRP5 inhibitor zaprinast had no effect on 6-MP uptake, efflux, or cytotoxicity, suggesting that MRP5 is not contributing to the 6-MP activity in this model. The MRP4 inhibitor ceefourin-1, however, significantly decreased the rate of efflux of 6-MP from SLC43A3-transfected HEK293 cells (Fig 8A), suggesting that MRP4 does contribute to 6-MP efflux in this model. This conjecture is supported by the finding

Molecular Pharmacology Fast Forward. Published on March 25, 2019 as DOI: 10.1124/mol.118.114389
This article has not been copyedited and formatted. The final version may differ from this version.

that transfection of the HEK293 cells with siRNA for ABCC4 led to an increase in their sensitivity to 6-MP at higher concentrations (Fig 10C). However, MRP4-mediated efflux of 6-MP is slower than that mediated by ENBT1, and only has an impact at lower levels of ENBT1 activity (such as when ENBT1 is partially inhibited with 100 μM adenine). The dominance of ENBT1 in this model is also apparent from the finding that ceefourin-1 had no effect on the cytotoxicity of 6-MP in SLC43A3-transfected cells (Fig 10). These data indicate that the compensatory downregulation of ABCC4 in the SLC43A3-transfected cells is not contributing to the enhanced sensitivity of the SLC43A3-transfected cells to 6-MP. Interestingly, incubation of the un-transfected HEK293 cells with MRP4 inhibitors resulted in a significant increase in the relative proportion of 6-MP resistant cells (Fig 10A). A similar trend was seen for the SLC43A3_1 transfected cells. MRP4 inhibition may lead to increased intracellular cAMP (an endogenous substrate for MRP4) causing cell cycle arrest, as has been reported in other cell lines (Copsel et al., 2011; Zhao et al., 2014), such that more of the cells enter a quiescent phase where they are not affected by 6-MP.

The significant contribution of ENBT1 to the cellular accumulation of 6-MP suggests that changes in the expression of this transporter may impact the therapeutic effectiveness of 6-MP. Little is known about the regulation of SLC43A3 expression. However, the striking downregulation (10-fold) of SLC43A3 expression in cells transfected with pcDNA3.1 only (vector control; Fig 3A), suggests that it is transcriptionally regulated. This decrease in expression also impacts the cellular sensitivity to 6-MP, as evidenced by a decrease in 6-MP cytotoxicity in the vector-transfected cells (Fig 9A). It is possible that metabolic stress associated with expression of aminoglycoside phosphotransferase (mediating the G418

Molecular Pharmacology Fast Forward. Published on March 25, 2019 as DOI: 10.1124/mol.118.114389
This article has not been copyedited and formatted. The final version may differ from this version.

resistance) in the transfected cells(Yallop and Svendsen, 2001; Veraitch and Al-Rubeai, 2005), and/or the chronic exposure to G418, may be responsible for this downregulation. We have shown previously that uptake of hypoxanthine by ENBT1 in microvascular endothelial cells is decreased by oxidative stress associated with hypoxia(Bone et al., 2014). This may have ramifications for use of nucleobase analogues in cancer therapy as there is a strong association between oxidative stress and cancer progression(Sosa et al., 2013).

Given the importance of ENBT1 to the cellular uptake of 6-MP, this system may be a target for drug-drug interactions which impact 6-MP therapeutic activity. Both isoforms (ENBT1.1 and ENBT1.2) had comparable sensitivities to the inhibitors tested (Fig 6). We confirmed that MTX and adenosine do not have affinity for ENBT1. MTX, as a folate analogue, would not be expected to inhibit ENBT1, but the confirmation of no direct drug-drug interactions via ENBT1 is important given that MTX is used in conjunction with 6-MP for chemotherapy. Likewise, the ENT1 blocker NBMPR was relatively ineffective against 6-MP uptake by ENBT1. The finding that adenosine and uridine had no inhibitory activity also confirms that ENT1, ENT2, CNT1, CNT2 and CNT3 are not involved in 6-MP uptake in our model. However, 2-chloroadenosine did significantly inhibit 6-MP uptake. This adenosine analog can induce apoptosis in B-cells, and is resistant to metabolism by adenosine deaminase (Bastin-Coyette et al., 2008) making it more metabolically stable than adenosine. 2-Chloroadenosine has also been reported to inhibit an ENBT1-like transporter in PK15-NTD (nucleoside transport deficient) cells (Hoque et al., 2008). It is possible that the addition of the halogen group leads to enhanced recognition by nucleobase transporters. In this regard, 2-chloroadenosine has higher affinity for the nucleoside transporter ENT2 than it does for ENT1 (Hammond, 1991), and ENT2 has a higher affinity for nucleobases

Molecular Pharmacology Fast Forward. Published on March 25, 2019 as DOI: 10.1124/mol.118.114389
This article has not been copyedited and formatted. The final version may differ from this version.

than does ENT1 (Yao et al., 2011). This chemical characteristic may be something to consider in the search for selective inhibitors of ENBT1. Also of interest is the finding that the 6-MP metabolite generated through the methylation of 6-MP by TPMT, 6-methylmercaptopurine (MMP), inhibits ENBT1. ENBT1.1 is bidirectional in that it can also mediate the efflux of 6-MP from cells. Therefore, it is possible that removal of MMP from cells via ENBT1 may contribute to cellular resistance to 6-MP, depending on the relative affinity of MMP for the transporter compared with subsequent intracellular enzymatic processes. It may be of value in future studies to determine how intracellular MMP affects the rate of uptake of 6-MP. A complex interplay between these two systems may explain some of the variability seen in the assessment of TPMT-mediated metabolism of 6-MP (Karas-Kuzelicki and Mlinaric-Rascan, 2009; Chouchana et al., 2014). We have also determined that 6-TG inhibits 6-MP uptake and is itself a likely substrate for ENBT1. 6-TG is not as commonly used in maintenance therapy of ALL due to the greater toxicity associated with its use (Vora et al., 2006; Stork et al., 2010), but it is used for the treatment of inflammatory bowel diseases such as Crohn's Disease (Bar et al., 2013).

In summary, we have established that both variants of ENBT1 can mediate the transport of 6-MP and that increased SLC43A3 expression enhances the ability of 6-MP to induce cell death. There are no apparent differences in the ENBT1 variants in terms of their affinity for adenine or 6-MP. Further studies examining whether differences in SLC43A3 expression contribute to the variability in 6-MP effectiveness when used in the treatment of leukemia and inflammatory bowel disorders are clearly warranted.

Molecular Pharmacology Fast Forward. Published on March 25, 2019 as DOI: 10.1124/mol.118.114389
This article has not been copyedited and formatted. The final version may differ from this version.

ACKNOWLEDGEMENTS

This work was aided by the excellent technical support of Ms Monika Dabrowska. We thank Dr Elaine Leslie (Physiology, University of Alberta) for the generous gift of ABCC4 siRNA. Nicholas Ruel acknowledges support received for his graduate training from the Faculty of Medicine & Dentistry, University of Alberta.

AUTHORSHIP CONTRIBUTIONS

Participated in research design: Hammond, Nguyen, and Ruel

Conducted experiments: Nguyen, Ruel, and Vilas

Contributed new reagents or analytic tools: Vilas

Performed data analysis: Hammond, and Ruel

Wrote or contributed to the writing of the manuscript: Hammond, and Ruel

REFERENCES

Ansari M, Sauty G, Labuda M, Gagne V, Laverdiere C, Moghrabi A, Sinnett D and Krajinovic M (2009) Polymorphisms in multidrug resistance-associated protein gene 4 is associated with outcome in childhood acute lymphoblastic leukemia. *Blood* **114**:1383-1386.

Bar F, Sina C and Fellermann K (2013) Thiopurines in inflammatory bowel disease revisited. *World J Gastroenterol* **19**:1699-1706.

Bastin-Coyette L, Smal C, Cardoen S, Saussoy P, Van den Neste E and Bontemps F (2008) Mechanisms of cell death induced by 2-chloroadenosine in leukemic B-cells. *Biochem Pharmacol* **75**:1451-1460.

Bodoy S, Fotiadis D, Stoeger C, Kanai Y and Palacin M (2013) The small SLC43 family: facilitator system l amino acid transporters and the orphan EEG1. *Mol Aspects Med* **34**:638-645.

Bone DB, Antic M, Vilas G and Hammond JR (2014) Oxidative stress modulates nucleobase transport in microvascular endothelial cells. *Microvasc Res* **95C**:68-75.

Bone DB and Hammond JR (2007) Nucleoside and nucleobase transporters of primary human cardiac microvascular endothelial cells: characterization of a novel nucleobase transporter. *Am J Physiol Heart Circ Physiol* **293**:H3325-3332.

Burckhardt G (2012) Drug transport by Organic Anion Transporters (OATs). *Pharmacol Ther* **136**:106-130.

Chen ZS, Lee K and Kruh GD (2001) Transport of cyclic nucleotides and estradiol 17-beta-D-glucuronide by multidrug resistance protein 4. Resistance to 6-mercaptopurine and 6-thioguanine. *J Biol Chem* **276**:33747-33754.

Cheng Y and Prusoff WH (1973) Relationship between the inhibition constant (K1) and the concentration of inhibitor which causes 50 per cent inhibition (I50) of an enzymatic reaction. *Biochem Pharmacol* **22**:3099-3108.

Chouchana L, Narjoz C, Roche D, Golmard JL, Pineau B, Chatellier G, Beaune P and Loriot MA (2014) Interindividual variability in TPMT enzyme activity: 10 years of experience with thiopurine pharmacogenetics and therapeutic drug monitoring. *Pharmacogenomics* **15**:745-757.

Copsel S, Garcia C, Diez F, Vermeulem M, Baldi A, Bianciotti LG, Russel FGM, Shayo C and Davio C (2011) Multidrug Resistance Protein 4 (MRP4/ABCC4) Regulates cAMP Cellular Levels and Controls Human Leukemia Cell Proliferation and Differentiation. *The Journal of Biological Chemistry* **286**:6979-6988.

Duan P and You G (2009) Novobiocin Is a Potent Inhibitor for Human Organic Anion Transporters. *Drug Metabolism and Disposition* **37**:1203-1210.

Fukuda Y and Schuetz JD (2012) ABC transporters and their role in nucleoside and nucleotide drug resistance. *Biochem Pharmacol* **83**:1073-1083.

Furukawa J, Inoue K, Maeda J, Yasujima T, Ohta K, Kanai Y, Takada T, Matsuo H and Yuasa H (2015) Functional identification of SLC43A3 as an equilibrative nucleobase transporter involved in purine salvage in mammals. *Sci Rep* **5**:15057.

Griffith DA and Jarvis SM (1993) High affinity sodium-dependent nucleobase transport in cultured renal epithelial cells (LLC-PK$_1$). *J Biol Chem* **268**:20085-20090.

Hammond JR (1991) Comparative pharmacology of the nitrobenzylthioguanosine-sensitive and -resistant nucleoside transport mechanisms of Ehrlich ascites tumor cells. *J Pharmacol Exp Ther* **259**:799-807.

Hoque KM, Chen L, Leung GP and Tse CM (2008) A purine-selective nucleobase/nucleoside transporter in PK15NTD cells. *Am J Physiol Regul Integr Comp Physiol* **294**:R1988-R1995.

Janke D, Mehralivand S, Strand D, Godtel-Armbrust U, Habermeier A, Gradhand U, Fischer C, Toliat MR, Fritz P, Zanger UM, Schwab M, Fromm MF, Nurnberg P, Wojnowski L, Closs EI and Lang T (2008) 6-mercaptopurine and 9-(2-phosphonyl-methoxyethyl) adenine (PMEA) transport altered by two missense mutations in the drug transporter gene ABCC4. *Hum Mutat* **29**:659-669.

Karas-Kuzelicki N and Mlinaric-Rascan I (2009) Individualization of thiopurine therapy: thiopurine S-methyltransferase and beyond. *Pharmacogenomics* **10**:1309-1322.

Kingston RE, Chen CA and Rose JK (2003) Calcium phosphate transfection. *Current protocols in molecular biology* **Chapter 9**:Unit 9.1.

Mori S, Ohtsuki S, Takanaga H, Kikkawa T, Kang YS and Terasaki T (2004) Organic anion transporter 3 is involved in the brain-to-blood efflux transport of thiopurine nucleobase analogs. *J Neurochem* **90**:931-941.

Nagai K, Nagasawa K, Kihara Y, Okuda H and Fujimoto S (2007) Anticancer nucleobase analogues 6-mercaptopurine and 6-thioguanine are novel substrates for equilibrative nucleoside transporter 2. *Int J Pharm* **333**:56-61.

Omasits U, Ahrens CH, Muller S and Wollscheid B (2014) Protter: interactive protein feature visualization and integration with experimental proteomic data. *Bioinformatics* **30**:884-886.

Peng XX, Shi Z, Damaraju VL, Huang XC, Kruh GD, Wu HC, Zhou Y, Tiwari A, Fu L, Cass CE and Chen ZS (2008) Up-regulation of MRP4 and down-regulation of influx

transporters in human leukemic cells with acquired resistance to 6-mercaptopurine. *Leuk Res* **32**:799-809.

Reid G, Wielinga P, Zelcer N, De Haas M, Van Deemter L, Wijnholds J, Balzarini J and Borst P (2003) Characterization of the transport of nucleoside analog drugs by the human multidrug resistance proteins MRP4 and MRP5. *Mol Pharmacol* **63**:1094-1103.

Senyavina NV and Tonevitskaya SA (2015) Effect of Hypoxanthine on Functional Activity of Nucleoside Transporters ENT1 and ENT2 in Caco-2 Polar Epithelial Intestinal Cells. *Bull Exp Biol Med* **160**:160-164.

Sosa V, Moline T, Somoza R, Paciucci R, Kondoh H and ME LL (2013) Oxidative stress and cancer: an overview. *Ageing Res Rev* **12**:376-390.

Stork LC, Matloub Y, Broxson E, La M, Yanofsky R, Sather H, Hutchinson R, Heerema NA, Sorrell AD, Masterson M, Bleyer A and Gaynon PS (2010) Oral 6-mercaptopurine versus oral 6-thioguanine and veno-occlusive disease in children with standard-risk acute lymphoblastic leukemia: report of the Children's Oncology Group CCG-1952 clinical trial. *Blood* **115**:2740-2748.

Tanaka Y, Manabe A, Fukushima H, Suzuki R, Nakadate H, Kondoh K, Nakamura K, Koh K, Fukushima T, Tsuchida M, Koike K, Kiyokawa N, Noguchi E, Sumazaki R and Komiyama T (2015) Multidrug resistance protein 4 (MRP4) polymorphisms impact the 6-mercaptopurine dose tolerance during maintenance therapy in Japanese childhood acute lymphoblastic leukemia. *Pharmacogenomics J* **15**:380-384.

Thul PJ, Akesson L, Wiking M, Mahdessian D, Geladaki A, Ait Blal H, Alm T, Asplund A, Bjork L, Breckels LM, Backstrom A, Danielsson F, Fagerberg L, Fall J, Gatto L, Gnann C, Hober S, Hjelmare M, Johansson F, Lee S, Lindskog C, Mulder J, Mulvey CM,

Nilsson P, Oksvold P, Rockberg J, Schutten R, Schwenk JM, Sivertsson A, Sjostedt E, Skogs M, Stadler C, Sullivan DP, Tegel H, Winsnes C, Zhang C, Zwahlen M, Mardinoglu A, Ponten F, von Feilitzen K, Lilley KS, Uhlen M and Lundberg E (2017) A subcellular map of the human proteome. *Science* **356**.

Veraitch FS and Al-Rubeai M (2005) Enhanced growth in NS0 cells expressing aminoglycoside phosphotransferase is associated with changes in metabolism, productivity, and apoptosis. *Biotechnology and bioengineering* **92**:589-599.

Vora A, Mitchell CD, Lennard L, Eden TO, Kinsey SE, Lilleyman J, Richards SM, Medical Research C and National Cancer Research Network Childhood Leukaemia Working P (2006) Toxicity and efficacy of 6-thioguanine versus 6-mercaptopurine in childhood lymphoblastic leukaemia: a randomised trial. *Lancet* **368**:1339-1348.

Ward JL, Sherali A, Mo ZP and Tse CM (2000) Kinetic and pharmacological properties of cloned human equilibrative nucleoside transporters, ENT1 and ENT2, stably expressed in nucleoside transporter-deficient PK15 cells. Ent2 exhibits a low affinity for guanosine and cytidine but a high affinity for inosine. *J Biol Chem* **275**:8375-8381.

Yallop CA and Svendsen I (2001) The effects of G418 on the growth and metabolism of recombinant mammalian cell lines. *Cytotechnology* **35**:101-114.

Yamamoto S, Inoue K, Murata T, Kamigaso S, Yasujima T, Maeda JY, Yoshida Y, Ohta KY and Yuasa H (2010) Identification and functional characterization of the first nucleobase transporter in mammals: implication in the species difference in the intestinal absorption mechanism of nucleobases and their analogs between higher primates and other mammals. *J Biol Chem* **285**:6522-6531.

Yao SY, Ng AM, Cass CE, Baldwin SA and Young JD (2011) Nucleobase transport by human equilibrative nucleoside transporter 1 (hENT1). *J Biol Chem* **286**:32552-32562.

Young JD, Yao SY, Baldwin JM, Cass CE and Baldwin SA (2013) The human concentrative and equilibrative nucleoside transporter families, SLC28 and SLC29. *Mol Aspects Med* **34**:529-547.

Zhao X, Guo Y, Yue W, Zhang L, Gu M and Wang Y (2014) ABCC4 is required for cell proliferation and tumorigenesis in non-small cell lung cancer. *OncoTargets and therapy* **7**:343-351.

Zhou M, Duan H, Engel K, Xia L and Wang J (2010) Adenosine transport by plasma membrane monoamine transporter: reinvestigation and comparison with organic cations. *Drug Metab Dispos* **38**:1798-1805.

Zhou M, Xia L, Engel K and Wang J (2007) Molecular determinants of substrate selectivity of a novel organic cation transporter (PMAT) in the SLC29 family. *J Biol Chem* **282**:3188-3195.

Molecular Pharmacology Fast Forward. Published on March 25, 2019 as DOI: 10.1124/mol.118.114389
This article has not been copyedited and formatted. The final version may differ from this version.

Footnotes

This work was supported by funding to JRH from the Cancer Research Society (Canada) [Grant #21355]

Figure Legends

Figure 1 – Predicted topology of ENBT1. Sequence shown is for the protein encoded by SLC43A3_1 (ENBT1.1). The 13 amino acid insert in ENBT1.2 (encoded by SLC43A3_2) after the alanine at position 61 is indicated. Structure was generate with Protter (http://wlab.ethz.ch/protter/start/) (Omasits et al., 2014).

Figure 2 – **Stable transfection of HEK293 cells with SLC43A3_1 and SLC43A3_2.** **A)** Transfection of HEK293 cells with SLC43A3 was confirmed using PCR with the RT-PCR primers specific for SLC43A3 (top) and GAPDH (bottom) shown in Table S1. cDNA was prepared from Total RNA isolated from un-transfected cells (HEK293) or HEK293 cells stably transfected with SLC43A3_1 or SLC43A3_2. **B)** Membranes were prepared from HEK293 cells and cells transfected with SLC43A3_1 (ENBT1.1) and SLC43A3_2 (ENBT1.2). Samples were resolved on SDS-PAGE gels, transferred to polyvinyl membranes and probed with anti-SLC43A3 and anti-β-actin antibodies. C) Parallel immunoblot analyses were performed as described above, but using anti-myc and anti-β-actin antibodies.

Figure 3. Compensatory changes in gene expression upon transfection of HEK293 cells with SLC43A3. Gene expression, assessed by qPCR, is shown relative to the amount detected in un-transfected HEK293 cells. Expression was normalized to GAPDH transcript levels in each individual experiment. **Panel A** shows the relative expression of SLC43A3 in HEK293 cells stably transfected with the respective SLC43A3_1, SLC43A3_2, or empty vector (pcDNA3.1) construct (N=5). **Panels B-D** show the relative expression of ENT1 (SLC29A1), ENT2 (SLC29A2), ENT4 (SLC29A4), MRP4 (ABCC4), MRP5 (ABCC5) and the enzymes TPMT and

Molecular Pharmacology Fast Forward. Published on March 25, 2019 as DOI: 10.1124/mol.118.114389
This article has not been copyedited and formatted. The final version may differ from this version.

HPRT in HEK293 cells transfected with either 'empty' pcDNA3.1 (B), SLC43A3_1 (**C**) or SLC43A3_2 (**D**). Bars represent the mean ± SD of 5 independent samples. * Significant difference in expression between un-transfected HEK293 cells and transfected HEK293 cells (Student's t-test, $P<0.05$, corrected for multiple comparisons with the Holm-Sidak method).

Figure 4. [^{3}H]Adenine transport by SLC43A3-encoded ENBT1. HEK293 cells and cells transfected with SLC43A3_1 (**A**), SLC43A3_2 or the empty pcDNA3.1 vector (**B**) were incubated with 100 μM [^{3}H]adenine at room temperature for the specified times (abscissa) and then centrifuged through oil. Cell pellets were digested overnight in 1 M NaOH and assessed for [^{3}H] content using standard liquid scintillation counting techniques to define pmol adenine accumulated per μl cell pellet (ordinate). ENBT1-mediated uptake was defined as the difference in cellular accumulation by the SLC43A3-transfected cells (SLC43A3-HEK293) and that observed in the un-transfected HEK293 cells assessed in parallel. Data points represent the mean ± SD of 6 (Panel A) or 5 (Panel B) experiments done in duplicate. **C)** The kinetics of ENBT1.1- and ENBT1.2-mediated uptake of [^{3}H]adenine were determined by assessing the uptake of a range of concentrations of [^{3}H]adenine (abscissa) as described for Panels A and B. Initial rates of influx (ordinate) were estimated as the transporter-mediated uptake at 0.5 s extrapolated from time course profiles as shown in Panel A (ENBT1.1), or directly from the 2 s uptake time point (Panel B; ENBT1.2). Data shown are the mean ± SD of N=5 experiments.

Figure 5. [^{14}C]6-MP transport by SLC43A3-encoded ENBT1. HEK293 cells and cells transfected with SLC43A3_1 (**A**), SLC43A3_2 or empty pcDNA3.1 (**B**) were incubated with 100 μM (**A**) or 30 μM (**B**) [^{14}C]6-MP at room temperature, in the presence and absence of 1 mM

Molecular Pharmacology Fast Forward. Published on March 25, 2019 as DOI: 10.1124/mol.118.114389
This article has not been copyedited and formatted. The final version may differ from this version.

adenine, for the specified times (abscissa) and then centrifuged through oil. Cell pellets were digested overnight in 1 M NaOH and assessed for [^{14}C] content using standard liquid scintillation counting techniques to define pmol 6-MP accumulated per µl cell pellet (ordinate). Data points represent the mean ± SD of 7 (Panel A) or 5 (Panel B) experiments done in duplicate. **C)** The kinetics of ENBT1.1- and ENBT1.2-mediated [^{14}C]6-MP uptake were determined by assessing the uptake of a range of concentrations of [^{14}C]6-MP (abscissa) as described for Panels A and B. Initial rates of influx (ordinate) were estimated as the transporter-mediated uptake (calculated as the difference in cellular uptake ± adenine) at 0.5 s interpolated from time course profiles as shown in Panel A (ENBT1.1), or directly from the 2 s uptake time point (ENBT1.2). Data shown are the mean ± SD of N=5 experiments.

Figure 6. Inhibition of [^{14}C]6-MP transport by SLC43A3-transfected HEK293 cells. The uptake of [^{14}C]6-MP by ENBT1.1 (100 µM; **Panel A**) and ENBT1.2 (30 µM; **Panel B**) was assessed using a 2 s time point in the presence and absence of the indicated concentration of methotrexate (MTX), 6-thioguanine (6-TG), 6-methylmercaptopurine (MMP), 2-chloroadenosine (2Cl-Ado), adenosine(Ado), 2-deoxyadenosine(Deoxy-Ado), hypoxantine (Hypox), uridine, nitrobenzylthioinosine (NBMPR), or decynium-22 (D22). Data were normalized as percent of control uptake where 100% was defined as the uptake [^{14}C]6-MP in the absence of inhibitor and 0% was defined as the uptake in the presence of 1 mM adenine. Each bar represents the mean ± SD of 5 experiments done in duplicate. * Significantly different from 100% control (Student's t-test, $P<0.05$, corrected for multiple comparisons with the Holm-Sidak method). **C)** Time courses were constructed at various concentrations of [^{3}H]adenine, as described for Figure 4C, in the presence of 750 µM 6-TG. Initial rates of transport were derived

Molecular Pharmacology Fast Forward. Published on March 25, 2019 as DOI: 10.1124/mol.118.114389
This article has not been copyedited and formatted. The final version may differ from this version.

from the rate of uptake at 0.5 s as extrapolated from the time course profiles. The dashed line indicates the analogous data obtained in the absence of 6-TG (from Figure 4C). Data points represent mean ± SD of 5 experiments done in duplicate. **D)** A range of concentrations of 6-TG, MMP, and D22 were assessed for their ability to inhibit the 2 s uptake of 100 μM [^{14}C]6-MP by the ENBT1.1. Data was normalized as percent of control uptake with 100% defined as the uptake of 100 μM [^{14}C]6-MP in the absence of inhibitor and 0% defined as that in the presence of 1 mM adenine. Sigmoid curves were fitted to these data for the determination of IC_{50} values which were used to calculate the inhibitor K_i values shown in the text. Each point represents the mean ± SD of N=5 experiments done in duplicate.

Figure 7. 6-MP efflux by ENBT1.1. A) Cells were loaded with 100 μM [^{14}C]6-MP for 30 s (SLC43A3_1 transfected) or 10 min (un-transfected HEK293), pelleted and then, to initiate efflux, suspended in either NMG buffer (Control) or buffer containing either 1 mM or 100 μM adenine. Aliquots of cell suspension were centrifuged through an oil layer at the specified times (abscissa) and processed to assess intracellular [^{14}C] content. Data are expressed as % of initial [^{14}C]6-MP load (ordinate) with 100% defined as [^{14}C]6-MP content at zero time extrapolated from curves fit (one phase exponential decay) to the 1 mM adenine data. One-phase or two-phase decay profiles were fitted to the data depending on which fit was determined to be statistically superior ($P < 0.05$; F-test). Each point represents the mean ± SD of 5 (Control and 100 μM adenine) or 10 (1 mM adenine) experiments.

Figure 8. Effect of ceefourin-1, zaprinast, and DY on 6-MP efflux. SLC43A3_1 transfected HEK293 cells were loaded with 100 μM [^{14}C]6-MP for 30 s pelleted and then, to initiate efflux,

suspended in either NMG buffer (Control) or buffer containing either 1 mM or 100 μM adenine, as indicated, in the presence and absence of the MRP4 inhibitor ceefourin-1 (50 μM; **A**), the MRP5 inhibitor zaprinast (100 μM; **B**), a combination of 50 μM ceefourin-1 and 100 μM zaprinast (**C**), or the ENT2 inhibitor DY (1 μM; **D**) . Aliquots of cell suspension were centrifuged through an oil layer at the specified times (abscissa) and processed to assess intracellular [^{14}C] content. Data are expressed as % of initial [^{14}C]6-MP load (ordinate), and either a one-phase or two-phase decay profile was fitted to the data based on which fit was determined to be statistically superior ($P < 0.05$; F-test). Each point represents the mean ± SD of 5 experiments.

Figure 9. SLC43A3 transfection of HEK293 cells significantly enhances the cytotoxicity of 6-MP. HEK293 cells and cells transfected with 'empty' pcDNA3.1 plasmid or SLC43A3_1 (**A**) or SLC43A3_2 (**B**) were plated at a density of 5 x 10^4 cells/well in 24-well plates and incubated with a range of concentrations of 6-MP (abscissa) for 48 hr at 37°C in a humidified incubator (5% CO_2/95% air). Cell viability was assessed using the MTT assay, and expressed as a percent of the cell viability measured at 48 hr in the absence of 6-MP (% of control; ordinate). Biphasic dose-response curves were fitted to these data using GraphPad Prism 7.02. Data points represent the mean ± SD of 5 experiments. * Significant difference between HEK293 cells and SLC43A3-transfected cells (Student's t-test, $P<0.05$, corrected for multiple comparisons with the Holm-Sidak method). **C)** Effect of DY on the cytotoxicity of 6-MP. HEK293 cells and cells transfected with SLC43A3_1 were incubated with a range of concentrations 6-MP in the absence and presence of the ENT1/ENT2 blocker DY (1 μM). Cell viability was assessed and data presented as described for Panels A & B (N=5). **D**) Effect of G418 on the cytotoxicity of 6-MP

Molecular Pharmacology Fast Forward. Published on March 25, 2019 as DOI: 10.1124/mol.118.114389
This article has not been copyedited and formatted. The final version may differ from this version.

in SLC43A3_1- and SLC43A3_2-transfected HEK293 cells. Cell viability was assessed upon incubation with the indicated concentrations of 6-MP for 48 h, as described for Panels A & B, in the presence and absence of G418 (N=5)

Figure 10. Effect of MRP4 and MRP5 inhibition on the cytotoxicity of 6-MP. HEK293 cells (**A**) and cells transfected with SLC43A3_1 (**B**) were exposed to a range of concentrations of 6-MP for 48 hr in the absence (Control) and presence of ceefourin-1 (50 μM), zaprinast (100 μM), or a combination of both, and then assessed for cell viability as described for Figure 9. * Significant difference between Control and ceefourin-1 + zaprinast. # Significant difference between Control and ceefourin-1 alone (Student's t-test, $P<0.05$, corrected for multiple comparisons with the Holm-Sidak method, N=6). **C)** HEK293 cells and cells transfected with SLC43A3_1 were stably transfected with ABCC4 (MRP4)-targeted siRNA. The cytotoxicity of a range of concentrations of 6-MP was then assessed in these cells lines as described for Figure 9. * Significant effect of siRNA in SLC43A3_1 transfected HEK293 cells. # Significant effect of siRNA in un-transfected HEK293 cells (Student's t-test, $P<0.05$, corrected for multiple comparisons with the Holm-Sidak method, N=5). **D)** ABCC4 transcript levels (± siRNA transfection) in the un-transfected and SLC43A3_1-transfected HEK293 cells used for the experiments shown in Panel C. GAPDH transcript levels were determined in parallel for each cell line to correct for loading differences. Densitometry analysis indicates that ABCC4 transcript was suppressed by ~60% in the siRNA transfected cells.

Molecular Pharmacology Fast Forward. Published on March 25, 2019 as DOI: 10.1124/mol.118.114389
This article has not been copyedited and formatted. The final version may differ from this version.

MOL # 114389

Figure 1

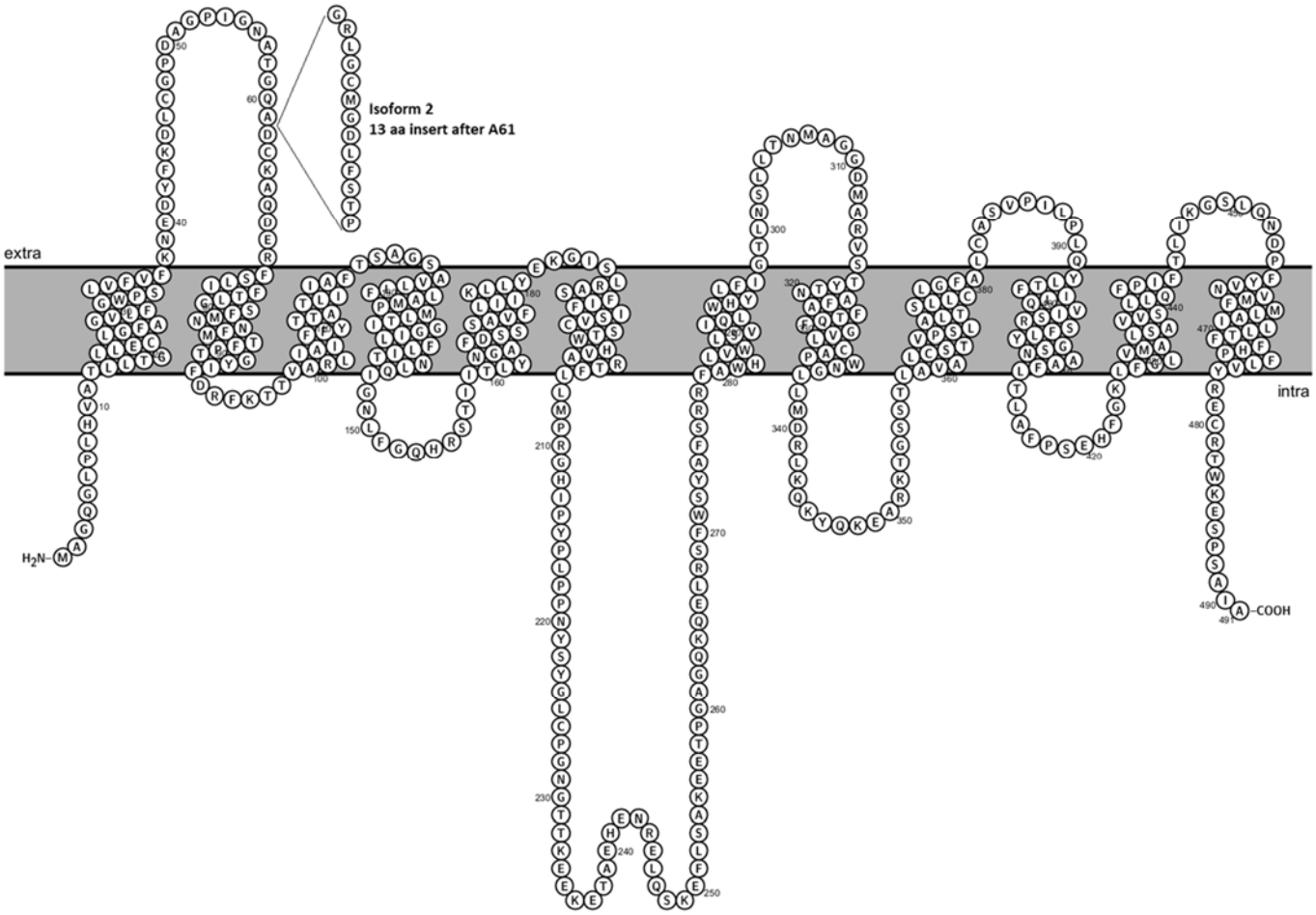

Molecular Pharmacology Fast Forward. Published on March 25, 2019 as DOI: 10.1124/mol.118.114389
This article has not been copyedited and formatted. The final version may differ from this version.

Figure 2

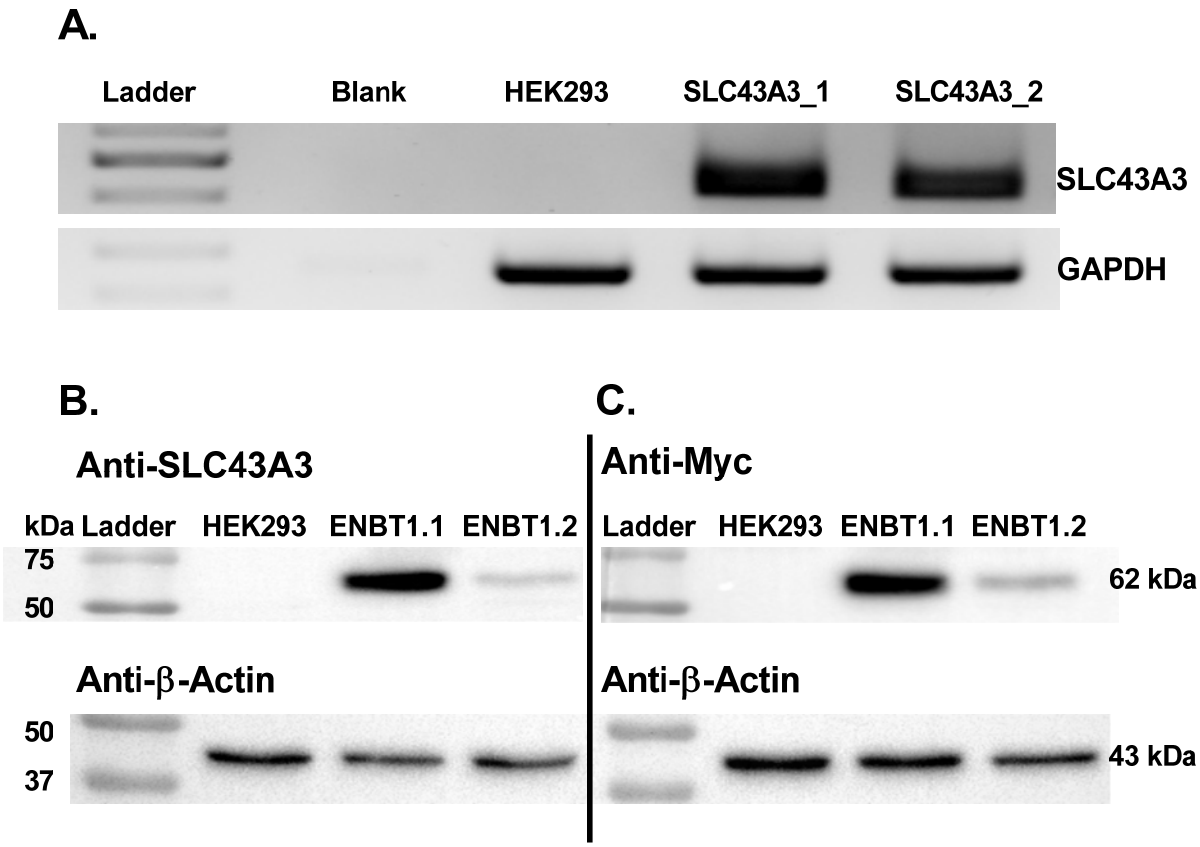

Molecular Pharmacology Fast Forward. Published on March 25, 2019 as DOI: 10.1124/mol.118.114389
This article has not been copyedited and formatted. The final version may differ from this version.

Figure 3

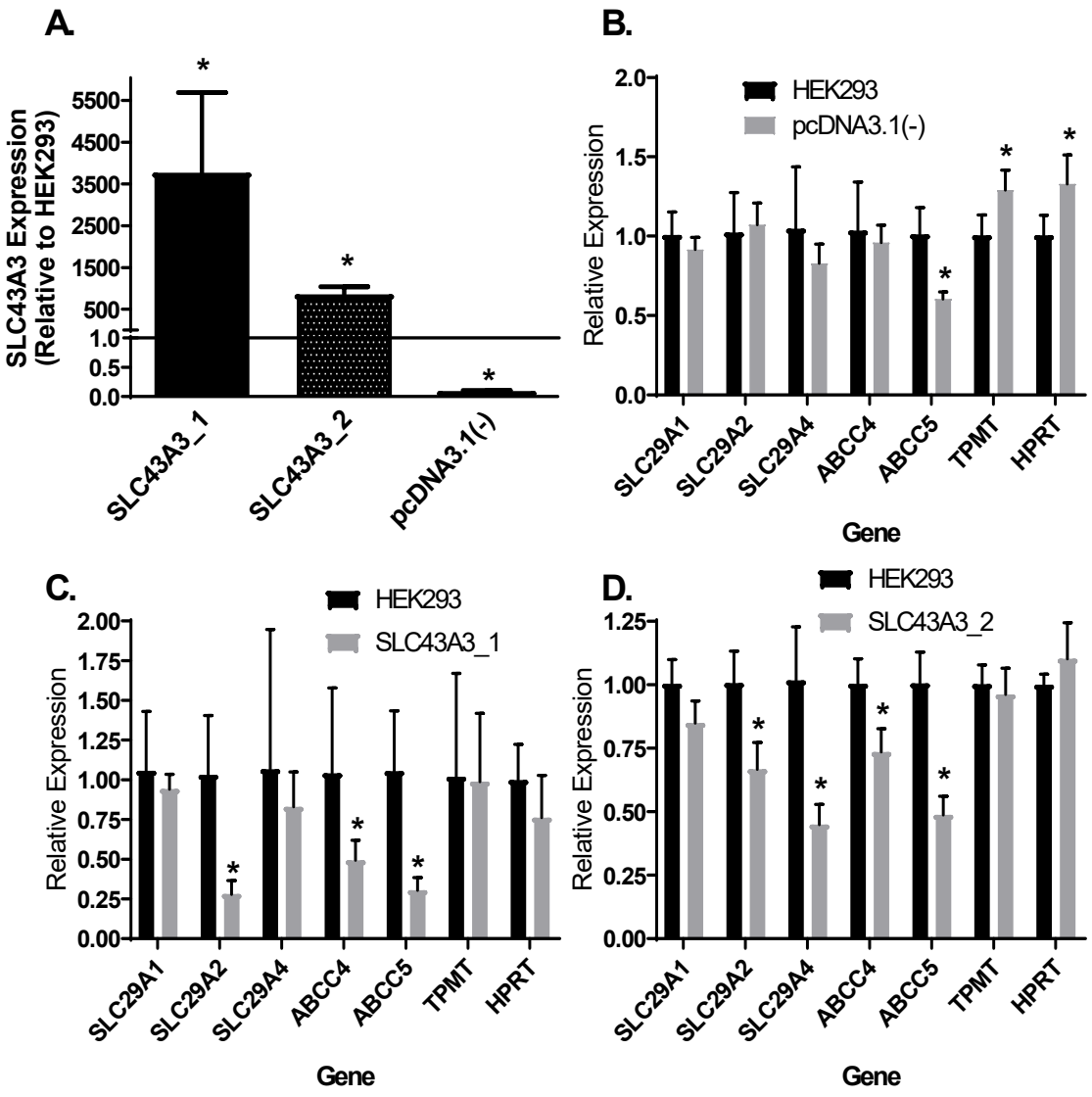

Molecular Pharmacology Fast Forward. Published on March 25, 2019 as DOI: 10.1124/mol.118.114389
This article has not been copyedited and formatted. The final version may differ from this version.

Figure 4

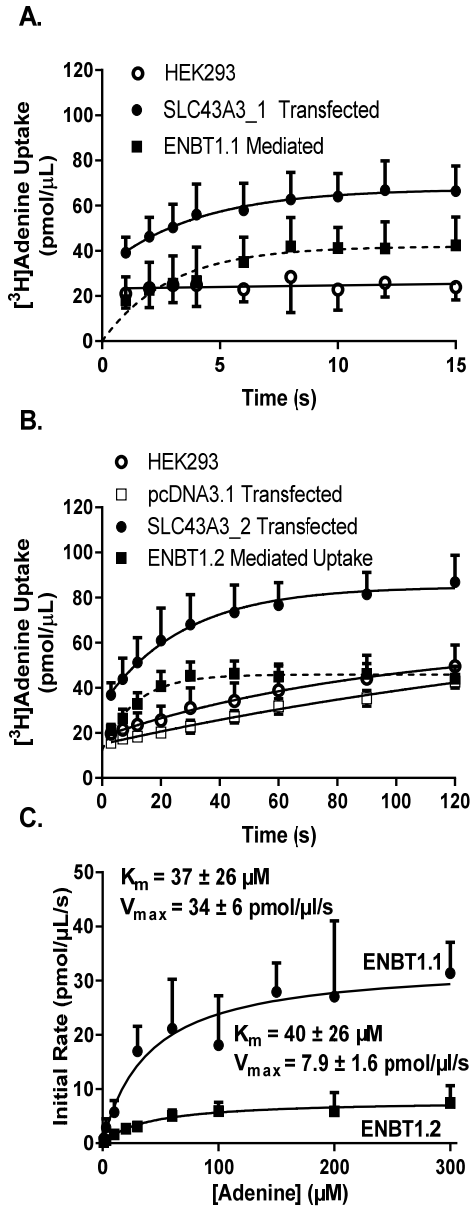

Molecular Pharmacology Fast Forward. Published on March 25, 2019 as DOI: 10.1124/mol.118.114389
This article has not been copyedited and formatted. The final version may differ from this version.

Figure 5

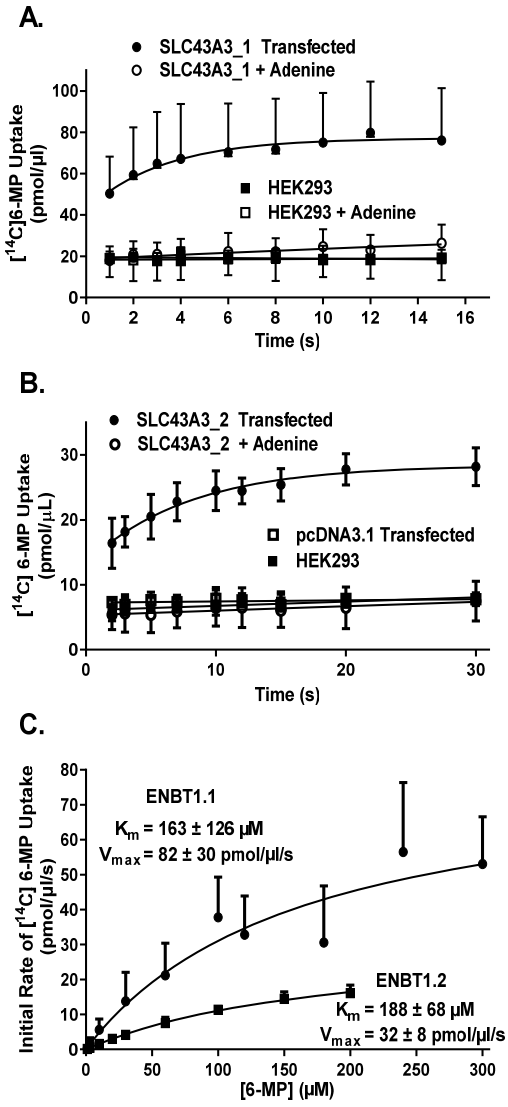

Molecular Pharmacology Fast Forward. Published on March 25, 2019 as DOI: 10.1124/mol.118.114389
This article has not been copyedited and formatted. The final version may differ from this version.

Figure 6

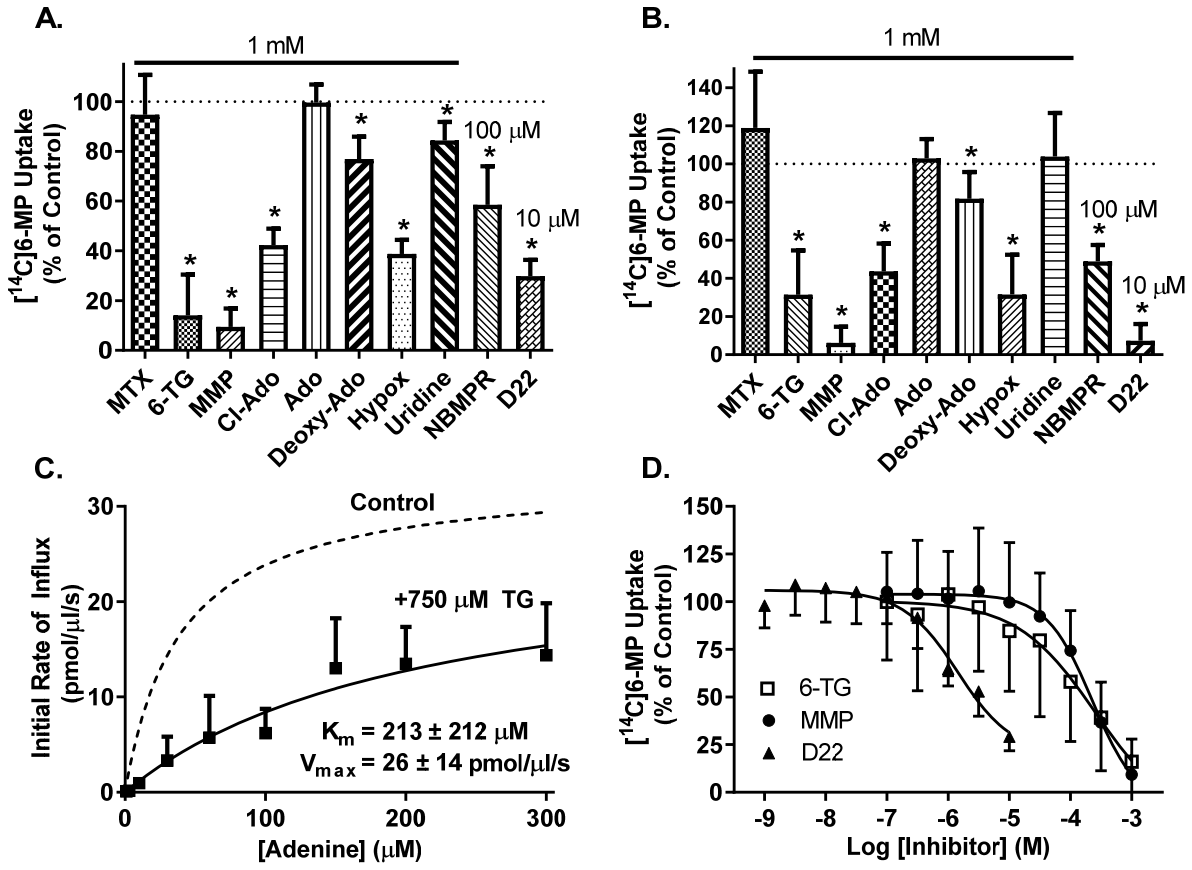

Molecular Pharmacology Fast Forward. Published on March 25, 2019 as DOI: 10.1124/mol.118.114389
This article has not been copyedited and formatted. The final version may differ from this version.

Figure 7

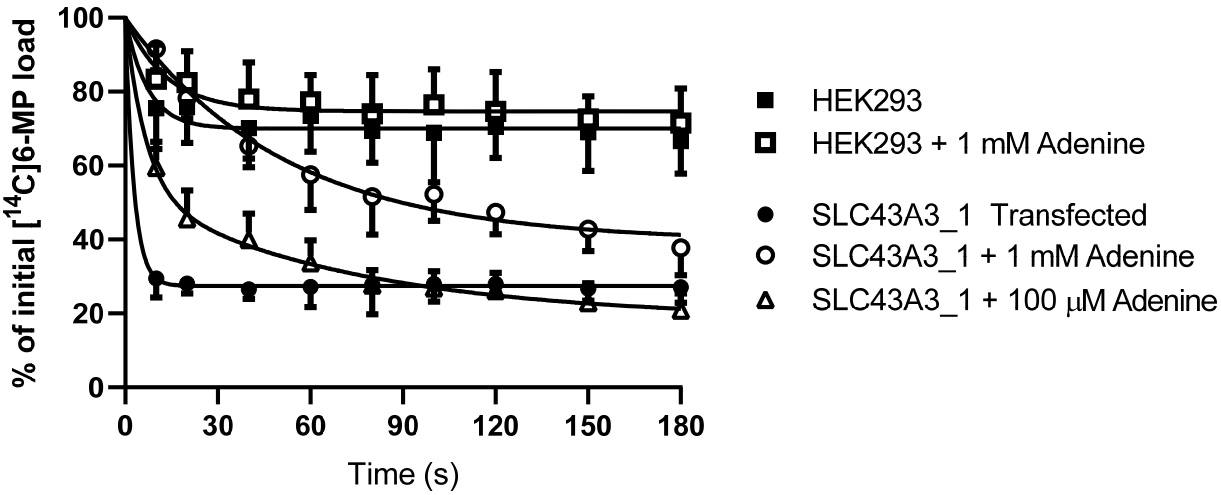

Molecular Pharmacology Fast Forward. Published on March 25, 2019 as DOI: 10.1124/mol.118.114389
This article has not been copyedited and formatted. The final version may differ from this version.

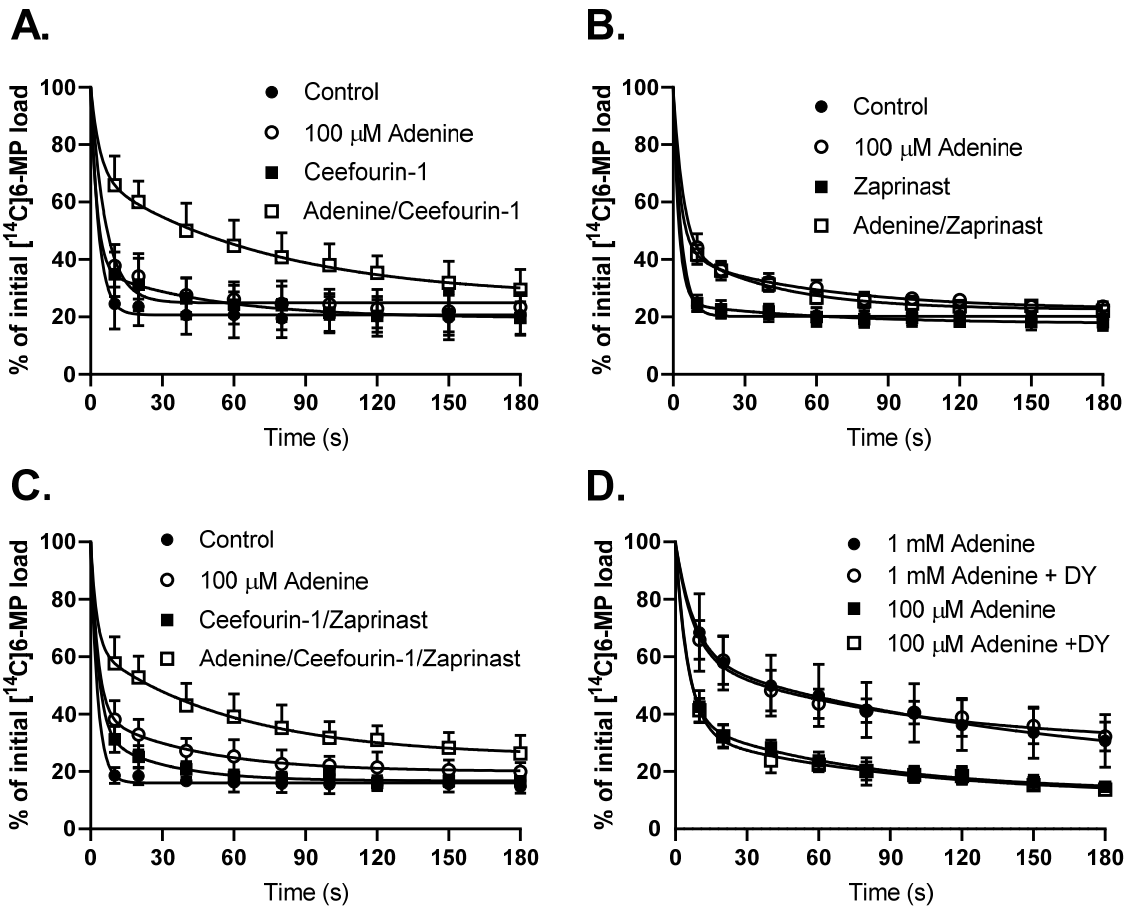

Figure 8

Molecular Pharmacology Fast Forward. Published on March 25, 2019 as DOI: 10.1124/mol.118.114389
This article has not been copyedited and formatted. The final version may differ from this version.

Figure 9

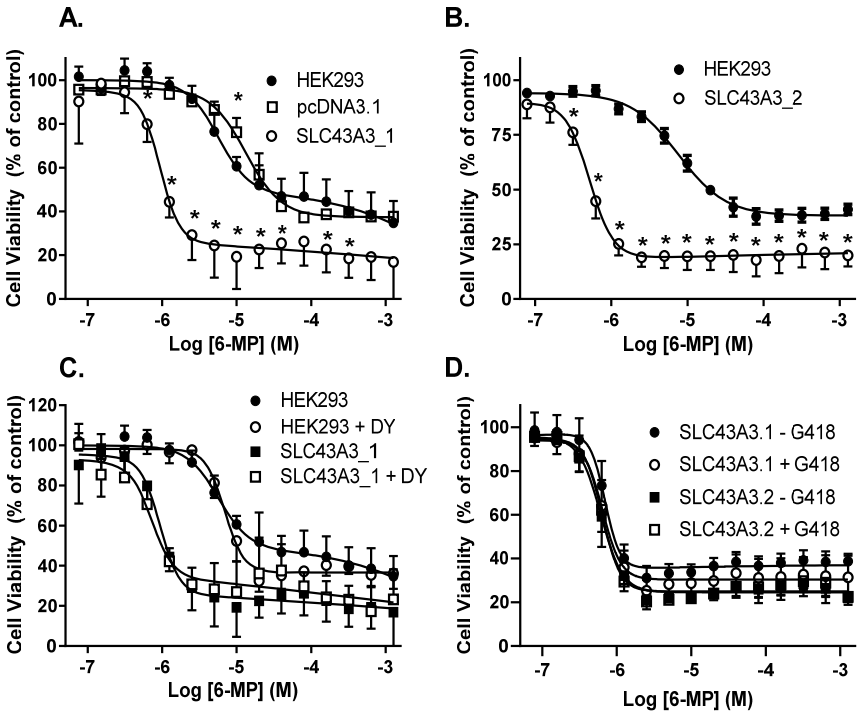

Molecular Pharmacology Fast Forward. Published on March 25, 2019 as DOI: 10.1124/mol.118.114389
This article has not been copyedited and formatted. The final version may differ from this version.

Figure 10